RESEARCH ARTICLE

Evaluation of lumbar spinal fusion utilizing recombinant human platelet derived growth factor-B chain homodimer (rhPDGF-BB) combined with a bovine collagen/β-tricalcium phosphate (β-TCP) matrix in an ovine model

Benjamin C. Gadomski[1] ![ORCID] | Kevin M. Labus[1] | Christian M. Puttlitz[1] ![ORCID] |
Kirk C. McGilvray[1] | Daniel P. Regan[2] | Brad Nelson[3] | Howard B. Seim III[3] |
Jeremiah T. Easley[3]

[1]Orthopaedic Bioengineering Research Laboratory, Department of Mechanical Engineering and School of Biomedical Engineering, Colorado State University, Fort Collins, Colorado, USA

[2]Department of Microbiology, Immunology, and Pathology, Colorado State University, Fort Collins, Colorado, USA

[3]Preclinical Surgical Research Laboratory, Department of Clinical Sciences, Colorado State University, Fort Collins, Colorado, USA

Correspondence
Jeremiah T. Easley, Preclinical Surgical Research Laboratory, Department of Clinical Sciences, Colorado State University, Fort Collins, CO, USA.
Email: jeremiah.easley@colostate.edu

Abstract

Background context: While the clinical effectiveness of recombinant human Platelet Derived Growth Factor-B chain homodimer combined with collagen and β-tricalcium phosphate (rhPDGF-BB + collagen/β-TCP) treatment for indications involving hindfoot and ankle is well-established, it is not approved for use in spinal interbody fusion, and the use of autograft remains the gold standard.

Purpose: The purpose of this study was to compare the effects of rhPDGF-BB + collagen/β-TCP treatment on lumbar spine interbody fusion in an ovine model to those of autograft bone and collagen/β-TCP treatments using biomechanical, radiographic, and histological assessment techniques.

Study design: Thirty-two skeletally mature Columbian Rambouillet sheep were used to evaluate the safety and effectiveness of rhPDGF-BB + collagen/β-TCP matrix in a lumbar spinal fusion model. Interbody polyetheretherketone (PEEK) cages contained either autograft, rhPDGF-BB + collagen/β-TCP, collagen/β-TCP matrix, or left empty.

Methods: Animals were sacrificed 8- or 16-weeks post-surgery. Spinal fusion was evaluated via post-sacrifice biomechanical, micro-computed tomography (μCT), and histological analysis. Outcomes were statistically compared using a two-way analysis of variance (ANOVA) with an alpha value of 0.05 and a Tukey post-hoc test.

Results: There were no statistically significant differences between groups within treatment timepoints for flexion-extension, lateral bending, or axial rotation range of motion, neutral zone, neutral zone stiffness, or elastic zone stiffness. μCT bone volume fraction was significantly greater between treatment groups independent of timepoint where Autograft and rhPDGF-BB + collagen/β-TCP treatments demonstrated significantly greater bone volume fraction as compared to collagen/β-TCP ($P = .026$ and $P = .038$, respectively) and Empty cage treatments ($P = .002$ and $P = .003$, respectively). μCT mean bone density fraction was most improved in

rhPDGF-BB + collagen/β-TCP specimens at the 8 week and 16-week timepoints as compared to all other treatment groups. There were no statistically significant differences in histomorphometric measurements of bone, soft tissue, or empty space between rhPDGF-BB + collagen/β-TCP and autograft treatments.

Conclusions: The results of this study indicate that the use of rhPDGF-BB combined with collagen/β-TCP promotes spinal fusion comparable to that of autograft bone.

Clinical significance: The data indicate that rhPDGF-BB combined with collagen/β-TCP promotes spinal fusion comparably to autograft bone treatment and may offer a viable alternative in large animal spinal fusion. Future prospective clinical studies are necessary to fully understand the role of rhPDGF-BB combined with collagen/β-TCP in human spinal fusion healing.

1 | INTRODUCTION

Platelet derived growth factor-B chain homodimer (PDGF-BB) has been shown to possess positive regenerative properties within the skeletal system.[1-3] PDGF-BB is a polypeptide growth factor released from platelets and acts early in the wound healing cascade as a chemoattractant and mitogenic agent for both osteoprogenitor cells and differentiated osteoblasts.[1-4] Recent studies have shown that PDGF plays a crucial role in coupling angiogenesis to osteogenesis during bone formation and healing.[5-7] These properties make PDGF-BB's role vital in the recruitment and amplification of the osteoblast lineage cells and promoting healing at the bone fusion site.[8-10] Numerous preclinical studies have been performed to investigate the efficacy of recombinant human PDGF-BB (rhPDGF-BB) for bone growth and fusion. A study by Nash et al demonstrated improved callus density and volume as well as biomechanical strength when rabbit tibial osteotomies were locally treated with PDGF (0.15 mL of collagen containing 80 μg of PDGF) as compared to osteotomies that received 0.15 mL of collagen alone,[11] while rhPDGF-BB combined with collagen and β-tricalcium phosphate (β-TCP) increased mechanical strength of both tibial fractures in geriatric, osteoporotic rats[12] and femoral fractures in BB Wistar diabetic rats.[13] Additionally, rhPDGF-BB increased spine bone mineral density, bone mass, and osteoblast numbers as compared to animals in osteoporotic rats.[14]

Clinically, mixtures of rhPDGF-BB combined with β-TCP have been used extensively in the context of hindfoot and ankle arthrodesis. The efficacy of combined rhPDGF-BB + β-TCP/collagen treatment for hindfoot and ankle fusion was investigated in a controlled clinical study in which 63 patients received rhPDGF-BB/β-TCP/collagen treatment and were compared to 148 patients that received autograft (control) treatment.[15] Complete fusion of the treated joints was reported for 84% of rhPDGF-BB + collagen/β-TCP-treated patients as compared to 65% of autograft-treated patients 24 weeks post-surgery, and in 91% of rhPDGF-BB + collagen/β-TCP-treated patients as compared to 78% of autograft-treated patients 52 weeks

post-surgery.[15] A similar, but larger, clinical study further investigated the use of rhPDGF-BB/β-TCP for patients undergoing hindfoot and ankle arthrodesis.[9] One-year post-surgery, 88.3% (348/394) of joints treated with rhPDGF-BB/β-TCP were considered healed while 87.2% (177/203) of joints treated with autograft were considered healed. A recent subset analysis of this study showed that use of rhPDGF-BB/β-TCP may also mitigate potential variability in autograft quality related to patient age.[16] Joints in subjects over the age of 65 years treated with rhPDGF-BB/β-TCP had approximately 2 times the odds of fusion success at 24 weeks as those treated with autograft (Odds Ratio 2.03, $P = .008$).

While the clinical effectiveness of rhPDGF-BB/β-TCP treatment for indications involving hindfoot and ankle is well-established, rhPDGF-BB/β-TCP treatment is not approved for use in spinal interbody fusion. The current gold standard treatment for interbody spine fusion to treat spinal deformities and chronic pain involves the removal of the intervertebral disc and insertion of a spacer along with graft material between the vertebral bodies to support and enhance the bone growth and fusion.[17-19] Despite the ubiquity of this treatment, availability, and quality of bone autograft material and patient inconvenience caused by donor site morbidity are common limitations associated with spinal interbody fusion.[20,21] Given its success in promoting bone fusion in the hindfoot and ankle without the use of supplemental autograft material, rhPDGF-BB combined with collagen/β-TCP may provide a viable alternative to the use of autograft for spinal interbody fusions. To date, two studies have investigated the safety and effectiveness of rhPDGF-BB combined with collagen/β-TCP matrix specifically in vertebral bone augmentation and spine fusion. In a previous study, rhPDGF-BB combined with collagen/β-TCP directly injected into the lumbar vertebral body in a primate model resulted in significantly increased vertebral bone mineral density and more robust trabecular bone morphology as compared to animals treated with collagen/β-TCP alone.[22] Additionally, sheep that underwent lumbar interbody spinal fusion demonstrated similar fusion rates when treated with rhPDGF-BB combined with collagen/β-TCP

or autograft alone after 24 weeks of healing.[23] While these results are promising, a comprehensive assessment of rhPDGF-BB + collagen/β-TCP that includes a direct comparison to collagen/β-TCP treatment alone for spinal interbody fusion with sufficient sample sizes has not been performed. Thus, the purpose of this study was to compare the effects of rhPDGF-BB + collagen/β-TCP treatment on lumbar spine interbody fusion in an ovine model to those of autograft bone and collagen/β-TCP treatments using biomechanical, radiographic, and histological assessment techniques. We hypothesized that rhPDGF-BB combined with collagen/β-TCP would result in similar fusion outcomes as autograft bone and improved fusion as compared to collagen/β-TCP treatment alone.

2 | MATERIALS AND METHODS

This proof-of-concept study focused on a dose level of rhPDGF-BB at 0.3 mg/mL since previously reported dosing evaluations for rhPDGF-BB across various clinical and preclinical bone repair indications both in humans and other mammal species, including periodontal osseous defect repair,[24,25] long-bone fracture healing,[12,13] and dose validation for bony fusion of the hindfoot/ankle in large-scale randomized controlled clinical trials,[15,26] have all demonstrated no added benefit to applying higher dose levels of rhPDGF-BB to enhance bone healing.

This study was performed under approval from the Colorado State University Institutional Animal Care and Use Committee. Thirty-two skeletally mature (3-5 years of age, approximately 80 kg) Columbian Rambouillet ewes were used to evaluate the safety and efficacy of rhPDGF-BB combined with β-TCP/collagen matrix in a lumbar spinal fusion model. Florfenicol (20 mg/kg, subcutaneous (SQ), Phenylbutazone (1 g, oral (PO), and two fentanyl patches (100 and 50mcg, transdermal) were applied to all sheep 24 hours prior to surgery and maintained for 5 days. The auricular vein and artery were catheterized and anesthesia was induced with a combination of ketamine (3.3 mg/kg, intravenous [IV]) and diazepam (0.1 mg/kg, IV). Following anesthetic induction, the sheep were intubated with a cuffed endotracheal tube, placed in right lateral recumbency, and maintained on isoflurane (1.5%-3%) with 100% oxygen using positive pressure ventilation (20 cm H_2O) for the duration of the procedure. Animals were placed under general anesthesia. A left lateral retroperitoneal approach was taken to dissect the oblique abdominal muscles to the ventral muscle plane of the transverse processes to expose the L2 through L5 vertebrae. Annulotomies were performed on the L2-L3 and L4-L5 intervertebral discs, and pituitary rongeurs were used to remove the lateral aspects of the annulus fibrosis and nucleus pulposus. The vertebral endplates were prepared by distracting the intervertebral space and advancing a 6 mm drill bit through the intervertebral disc space and further removing the vertebral endplates with a high-speed cylindrical diamond burr to the size of the respective interbody implant. Interbody polyetheretherketone (PEEK) cages (VS1-8 [22 mm length × 12.80 mm width × 7.20 mm height with aperture volume of 1 cm³], Artemedics LLC, Minneapolis, Minnesota) contained one of four treatments: Group 1: cancellous autograft

harvested from the iliac crest (Autograft), Group 2: 0.3 mg/mL rhPDGF-BB combined with collagen /β-TCP matrix (rhPDGF-BB + collagen/β-TCP, 2:1 volume/mass ratio), Group 3: 20 mM sodium acetate solution vehicle combined with collagen/β-TCP matrix (2:1 volume/mass ratio) (collagen/β-TCP), or Group 4: empty PEEK interbody cage (Empty). Treatments were randomized among animals and spinal location; each animal received one of the four treatments at L2-L3 and a different treatment at L4-L5 levels. Following the insertion of the interbody implants, 4.5 mm × 30 mm polyaxial pedicle screws were placed in the center of cranial and caudal vertebral bodies in the dorsal plane and secured with precut titanium rods (5.5 mm × 80 mm) and locking caps (ARCAS-003, Artemedics LLC, Minneapolis, Minnesota). Sheep were allowed to move and eat ad libitum following recovery and were monitored daily over the course of the study for pain, lameness, ambulatory status, infection, neurological effects, and any other signs of complications.

Sixteen animals were sacrificed 8-weeks post-surgery and the remaining 16 animals were sacrificed 16 weeks post-surgery. Within each sacrifice timepoint, ten (n = 10) implant levels contained iliac crest autograft (Autograft Group), ten (n = 10) implant levels contained collagen/β-TCP-rhPDGF-BB test article (rhPDGF-BB + collagen/β-TCP Group), six (n = 6) implant levels contained collagen/β-TCP-sodium acetate vehicles without rhPDGF-BB (collagen/β-TCP Group), and six (n = 6) implant levels contained empty PEEK cages (Empty Group). Treatments were assigned using a fractional factorial block randomization technique and controlled so that no animal received two levels of the same treatment. Following sacrifice, lumbar spine sections were dissected into functional spinal units (FSUs) for ex vivo analysis with care taken to remove extraneous soft tissues while preserving structural soft tissues including the facet capsular ligaments, anterior longitudinal ligament, posterior longitudinal ligament, interspinous ligament, and supraspinous ligament. The pedicle screws and connecting rods were removed, and specimen hydration was maintained with phosphate buffered saline (PBS) spray at 10-minute intervals through the dissection and experimentation process.

2.1 | Non-destructive biomechanical testing

Following dissection, the cranial and caudal portions of each FSU were potted in a two-part hardening resin (SmoothCast 321, Smooth-On, Macungie, Pennsylvania) for fixation in the biomechanical testing system. Pure moments of ±6.0 Nm were applied to each FSU in the Flexion—Extension, Left Lateral—Right Lateral, and Left Axial—Right Axial principal directions using a custom-manufactured spinal testing system that consisted of a stepper motor actuator (Model: E1402000E701, Danaher Controls, Gurnee, Illinois) in a force-feedback loop with a separate torque sensor. Applied moments were measured with a six degree-of-freedom load transducer (AMTI, Watertown, Massachusetts) and recorded at 100 Hz using a custom-written code (Labview 2018, National Instruments Co., Austin, Texas). The magnitude of off-axis moments (mean ± SD) measured at 6 Nm of moment in the testing axis were 0.68 ± 0.40 Nm in flexion, 0.71 ± 0.53 Nm in extension, 0.66 ± 0.33 Nm in lateral bending, and 0.37

± 0.15 Nm in axial rotation. Spinal motion was quantified with a three-camera stereophotogrammetry system (Motion Analysis Corp., Santa Rosa, California) that tracked the three-dimensional motion of reflective marker triads attached to each vertebral body. Three-dimensional coordinates were recorded for the reflective triads at 100 Hz, and Euler angles for the implanted FSUs were calculated (Matlab, MathWorks, Natick, Massachusetts). All FSUs underwent five loading cycles for each bending direction for specimen preconditioning with reported data extracted from the final cycle. Kinematic range of motion (ROM, deg), neutral zone (NZ, deg), neutral zone stiffness (NZ stiffness, Nm/deg), and elastic zone stiffness (EZ stiffness, Nm/deg) were quantified for each FSU. ROM was calculated as the absolute difference between the maximum and minimum rotational angles measured during the final loading cycle. The limits of the neutral zone were defined at the locations where the second derivative of the angle were maximum and minimum.[27] The neutral zone was the range of rotation between these limits, and the neutral zone stiffness was calculated as the inverse of the slope of the moment-rotation curve within that range. The elastic zone stiffness was defined as the inverse of the slope of the moment-rotation curve at the maximum and minimum tested moments. Biomechanical testing was performed in a blinded fashion in which the testers were not aware of specimen treatment allocation during experimentation and were unblinded to specimen treatment after data post-processing. Specimens were transferred to 10% neutral buffered formalin (NBF) solution for fixation following biomechanical testing.

2.2 | Micro-computed tomography (μCT)

Micro-computed tomography (μCT) scanning was completed on all specimens following non-destructive biomechanical testing. Specimens were trimmed superior to the cranial pedicle screw hole and inferior to the caudal screw hole in the transverse plane. The resultant tissue sections encompassed both vertebral body endplates, the intervertebral disc/fusion space, the interbody device, and any callus formation. The specimens were scanned at a resolution of 37 μm (Scanco μCT 80, Scanco USA Inc., Wayne, Pennsylvania) and bone volume fraction (BV/TV), or the volume of bone within the region of interest (ROI) normalized to the total ROI volume, and bone density fraction (MDBV/MDTV), or the mean density of bone within the ROI normalized to the mean density of the total volume of the ROI were calculated. The ROI used for this analysis was the entire volume within the interbody PEEK cage. As BV/TV approaches 100% and MDBV/MDTV approaches unity, then the ROI is considered to have a more solid architecture. μCT analysis was performed in a blinded fashion in which the evaluator was not aware of specimen treatment allocation during scanning or analysis and was unblinded to specimen treatment after data post-processing.

2.3 | Histology preparation & histomorphometry

Undecalcified histological processing was performed on all samples following μCT scanning and fixation in 10% NBF. Specimens were

bisected in the sagittal plane to expose the intervertebral disc space, central region of the interbody PEEK cage, and cranial/caudal endplates. Each sagittally bisected specimen was then dehydrated in graded solutions of ethyl alcohol using an automated tissue processing system (ASP300S, Leica Biosystems, Buffalo Grove, Illinois) and cleared manually with methyl salicylate and xylene before being polymerized into hardened acrylic resin blocks (MMA). Prior to collecting histology sections, care was taken to ensure a minimum distance of >1 cm was represented between each histology slide mounted section. Histology slide mounted sections were cut from each of the two (2) bisected halves in the sagittal plane using the EXAKT Cutting and Grinding system (EXAKT Technologies, Inc., Oklahoma City, Oklahoma) to display the interbody PEEK cage and inner tissue constituents, surrounding bone, and vertebral body endplates. One (1) slide from each bisected specimen block for a total of two (2) slides per original vertebral body specimen were cut and stained with Sanderson's rapid bone stain followed by Van Gieson's stain as a counterstain.

Histomorphometric evaluation was performed on calibrated digital images of each histology slide to quantify the percentage of bone, soft tissue, and empty space within each interbody PEEK cage (Image Pro, Media Cybernetics, Silver Spring, Maryland). Stained histology slides were evaluated by a board-certified veterinary pathologist (blinded to treatment group) to semi-quantitatively evaluate the presence of cells (polymorphonuclear cells, lymphocytes, plasma cells, macrophages, giant cells, osteoblasts), responses (bone remodeling, implant degradation, neovascularization), and bone bridging. Histomorphometry and histopathology analyses were performed in a blinded fashion in which the evaluator or pathologist was not aware of specimen treatment allocation during analysis and was unblinded to specimen treatment after data post-processing.

2.4 | Statistical analysis

Statistical analyses were performed on biomechanical, μCT, and histomorphometric outcome parameters using a two-way analysis of variance (ANOVA) with a Tukey post-hoc test and an alpha (α) value of 0.05 (Minitab 17, Minitab, State College, Pennsylvania). Treatment group and sacrifice timepoint served as the levels of each statistical comparison. All data were included in statistical comparisons. Flexion-extension ROM, flexion-extension NZ, bone volume fraction, bone area, soft tissue area, and empty space area raw data satisfied the normality and equal variance assumptions of the statistical analysis. All other data underwent Box-Cox transformations in order to satisfy these assumptions. Data are presented in box and whisker plot format where the "box" is bounded by the first and third quartiles, the "whiskers" represent the maximum/minimum values within the data set, the horizontal line represents the data median, and mean data are represented by "x." Outlier data are represented by "•" and were calculated as the first quartile minus 1.5 times the interquartile range or the third quartile plus 1.5 times the interquartile range, are highlighted (Microsoft Excel 2016, Redmond, Washington).

TABLE 1 Biomechanical outcome parameters. No statistically significant differences in ROM, NZ, or stiffness were observed between treatment groups within the 8-week or 16-week timepoints. Lower ROM and NZ values and higher stiffness values indicate greater levels of fusion. Values are reported as means ± SD

Outcome Parameter	8-Week Timepoint				16-Week Timepoint			
	Autograft	rhPDGF-BB + Collagen/β-TCP	Collagen/β-TCP	Empty	Autograft	rhPDGF-BB + Collagen/β-TCP	Collagen/β-TCP	Empty
Flexion-Extension ROM (Degrees)	6.14 ± 1.71	5.45 ± 2.05	5.92 ± 3.71	5.83 ± 2.06	2.94 ± 1.67	2.21 ± 1.12	2.02 ± 1.38	3.24 ± 1.19
Flexion-Extension NZ (Degrees)	1.58 ± 0.58	1.36 ± 0.57	1.51 ± 1.21	1.59 ± 0.77	0.77 ± 0.56	0.74 ± 0.48	0.58 ± 0.40	0.83 ± 0.29
Flexion-Extension NZ Stiffness (Nm/Degree)	0.51 ± 0.41	2.16 ± 5.61	3.47 ± 7.37	0.63 ± 0.42	6.62 ± 9.53	5.90 ± 8.09	12.67 ± 23.18	1.86 ± 1.05
Flexion EZ Stiffness (Nm/Degree)	4.92 ± 1.00	13.72 ± 29.88	9.21 ± 12.14	5.13 ± 1.15	5.54 ± 2.42	7.37 ± 4.91	10.14 ± 9.49	4.80 ± 1.13
Extension EZ Stiffness (Nm/Degree)	5.90 ± 3.50	9.76 ± 10.84	14.04 ± 21.45	6.66 ± 2.98	19.89 ± 29.91	17.10 ± 10.17	38.38 ± 53.80	11.73 ± 7.48
Lateral Bending ROM (Degrees)	6.93 ± 2.21	6.17 ± 2.29	7.06 ± 2.15	5.67 ± 1.39	2.17 ± 2.81	1.33 ± 1.06	1.39 ± 0.57	2.03 ± 1.61
Lateral Bending NZ (Degrees)	1.57 ± 0.67	1.58 ± 0.61	1.73 ± 0.78	1.36 ± 0.32	0.52 ± 0.59	0.25 ± 0.25	0.28 ± 0.22	0.45 ± 0.40
Lateral Bending NZ Stiffness (Nm/Degree)	0.42 ± 0.28	2.40 ± 6.81	0.32 ± 0.12	0.52 ± 0.23	6.65 ± 5.34	12.95 ± 16.35	12.86 ± 13.20	7.67 ± 9.40
Lateral Bending EZ Stiffness (Nm/Degree)	3.70 ± 0.68	6.38 ± 8.58	4.00 ± 0.82	4.33 ± 1.44	12.72 ± 6.52	13.45 ± 7.58	12.09 ± 3.42	10.94 ± 7.23
Axial Rotation ROM (Degrees)	1.45 ± 0.58	1.46 ± 0.54	2.24 ± 1.56	1.36 ± 1.08	0.47 ± 0.20	0.37 ± 0.20	0.49 ± 0.22	0.55 ± 0.33
Axial Rotation NZ (Degrees)	0.42 ± 0.19	0.41 ± 0.22	0.68 ± 0.52	0.38 ± 0.30	0.11 ± 0.09	0.08 ± 0.06	0.10 ± 0.07	0.21 ± 0.15
Axial Rotation NZ Stiffness (Nm/Degree)	5.13 ± 2.91	15.70 ± 38.94	3.96 ± 2.82	26.55 ± 47.19	43.47 ± 33.57	36.89 ± 22.11	24.31 ± 9.70	28.07 ± 21.93
Axial Rotation EZ Stiffness (Nm/Degree)	14.19 ± 10.75	21.90 ± 36.91	9.33 ± 3.84	31.39 ± 44.73	30.37 ± 15.07	39.15 ± 19.43	32.57 ± 20.70	29.93 ± 13.21
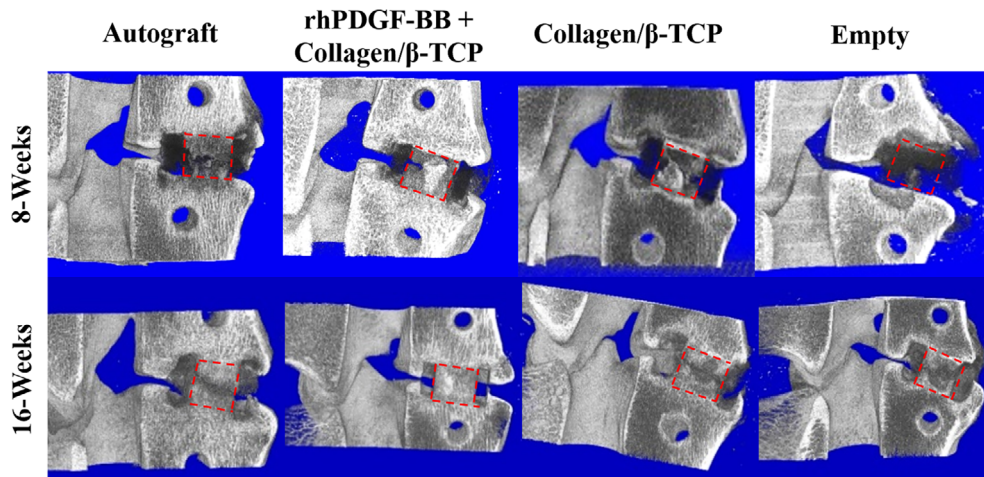
3 | RESULTS

Surgery was consistently performed across all animals. All animals recovered well from surgery without complication. All animals maintained appropriate weights and overall health appeared normal throughout the study. A single animal was treated for a mild conjunctivitis during the study period that resolved with appropriate therapy. All specimens were tested to completion, and no experimental issues, grossly abnormal spinal pathologies, ectopic bone formation, or abnormal tissue reactions were noted during dissection or testing.

3.1 | Non-destructive biomechanical testing

There were no statistically significant differences between treatment groups for flexion-extension, lateral bending, or axial rotation ROM, NZ, NZ stiffness, or EZ stiffness (Table 1). There were no statistically significant treatment-timepoint interaction effects in ROM, NZ, NZ stiffness, or EZ stiffness in any loading direction. The 16-week timepoint demonstrated significantly lower ROM and NZ as well as significantly greater NZ stiffness and EZ stiffness as compared to the 8-week timepoint for all motion directions across all treatments ($P < .001$) with the single exception of flexion EZ stiffness ($P = .41$).

3.2 | Micro-computed tomography (µCT)

Representative sagittal plane cross-sectional images through the center of the vertebral body of each treatment group at the 8-week and 16-week timepoints are presented in Figure 1. Greater bone volume fraction was observed for all 16-week specimens as compared to 8-week specimens; however, no statistically significant differences were observed within the 8 or 16-week timepoints ($P < .001$, Figure 2). Bone volume fraction was significantly greater between treatment groups independent of timepoint where Autograft and rhPDGF-BB + collagen/β-TCP treatments demonstrated significantly greater BV/TV as compared to collagen/β-TCP ($P = .026$ and

$P = .038$, respectively) and Empty cage treatments ($P = .002$ and $P = .003$, respectively).

rhPDGF-BB + collagen/β-TCP demonstrated the lowest mean bone density fraction value (ie, greatest amount of bone compaction) at the 8 week and 16-week timepoints as compared to all other treatment groups (Figure 2). Mean bone density fraction was significantly lower in 16-week specimens as compared to 8-week specimens overall ($P < .001$). No statistically significant differences were observed between specimens within the 8-week timepoint. Within 16-week specimens, the Autograft group demonstrated significantly improved mean bone density fraction as compared to the Empty group ($P = .021$), while the rhPDGF-BB + collagen/β-TCP group demonstrated significantly improved mean bone density fraction as compared to the collagen/β-TCP ($P < .001$) and Empty ($P < .001$) groups. There were no statistically significant differences in bone density fraction between the rhPDGF-BB + collagen/β-TCP and autograft groups at either timepoint.

3.3 | Histomorphometry

Representative histology images of each treatment group at the 8-week and 16-week timepoints are presented in Figure 3. Percent bone area was significantly greater at the 16-week timepoint as compared to the 8-week timepoint ($P < .001$, Figure 4A). Within timepoints, the Autograft group demonstrated significantly greater percent bone area as compared to the collagen/β-TCP group at 8-weeks ($P = .005$), and there were no other treatment-related differences. Overall, the Autograft group demonstrated significantly greater percent bone area as compared to the collagen/β-TCP and Empty groups, independent of treatment timepoint, but demonstrated no significant difference from the rhPDGF-BB+ collagen/β-TCP group. Again, percent soft tissue area was significantly greater at the 8-week timepoint as compared to the 16-week timepoint ($P < .001$, Figure 4B). Within the 8-week timepoint, the Autograft group demonstrated significantly lower percent soft tissue area as compared to the rhPDGF-BB + collagen/β-TCP ($P = .022$) and collagen/β-TCP
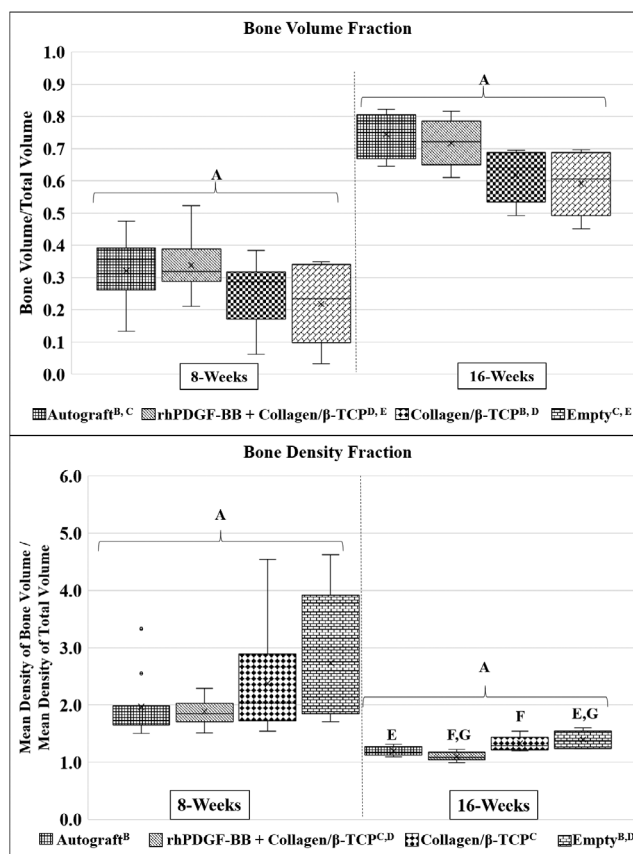
FIGURE 2 Quantitative three-dimensional μCT analysis was performed within the volume encapsulated by the PEEK interbody implant. Like roman numerals presented in the figure or figure legend indicate statistical differences. (Top) Bone volume fraction (BV/TV) was not significantly different between treatments groups within the 8-week or 16-week timepoints. Statistically significant overall main effects were observed between timepoints (16-week BV/TV was significantly greater than 8-week BV/TV, A: $P < .001$) and between treatment groups independent of timepoint where Autograft and rhPDGF-BB + collagen/β-TCP treatments demonstrated significantly greater BV/TV as compared to collagen/β-TCP (B: $P = .026$ and C: $P = .038$, respectively) and Empty cage treatments (D: $P = .002$ and E: $P = .003$, respectively). (Bottom) As bone density fraction (MDBV/MDTV) approaches unity, then the region of interest is considered to have a more solid architecture and is used to quantify the solidity of bone within the graft window. MDBV/MDTV was not significantly different between treatments at the 8-week timepoint. At the 16-week timepoint, rhPDGF-BB + collagen/β-TCP treatment demonstrated significantly improved MDBV/MDTV as compared to collagen/β-TCP and Empty cage treatments while Autograft treatment resulted in significantly improved MDBV/MDTV as compared to Empty cage treatment. Statistically significant overall main effects were observed between timepoint (16-week MDBV/MDTV was significantly lower than that at 8-weeks, A: $P < .001$) and between treatments independent of timepoint where MDBV/MDTV was significantly reduced in Autograft specimens as compared to collagen/β-TCP specimens (B: $P = .002$) and significantly reduced in rhPDGF + collagen/β-TCP as compared to collagen/β-TCP specimens (C: $P = .001$) and Empty cage specimens (D: $P < .001$). Data are presented in box and whisker plot format. The "box" is bounded by the first and third quartiles and were generated exclusive of median values in the event there was an odd number of data points (Microsoft Excel 2016, Redmond, Washington). The "whiskers" represent the maximum/minimum values within the data set; the horizontal line represents the data median, and mean data are represented by "x." Outlier data are represented by "•" and were calculated as the first quartile minus 1.5 times the interquartile range or the third quartile plus 1.5 times the interquartile range, are highlighted

($P < .001$) groups. Percent empty area was significantly greater at the 16-week timepoint as compared to the 8-week timepoint overall; however, there were no statistical differences between treatment groups within either timepoint ($P < .001$, (Figure 4C).

3.4 | Histopathology

Based on qualitative assessments of histology of all animals across the treatment groups, the degree of new bone formation and complete union/fusion of treated vertebral bodies increased at 16 weeks post-surgery for all animals, as compared to their respective groups at the 8-week timepoint (Figure 5). At the 8-week timepoint, new bone formation was greatest in the autograft group, followed in degree by the rhPDGF-BB + collagen/-TCP group and less new bone formation in the collagen/β-TCP alone group. At the 16-week timepoint, there were no differences in new bone formation/fusion in animals treated with autograft and rhPDGF-BB + collagen/β-TCP (>75%-100% new bone) and a moderate reduction in new bone formation in animals treated with collagen/β-TCP alone or no treatment (Empty group) (>50%-100% new bone).

| Autograft | rhPDGF-BB + Collagen/β-TCP | Collagen/β-TCP | Empty |
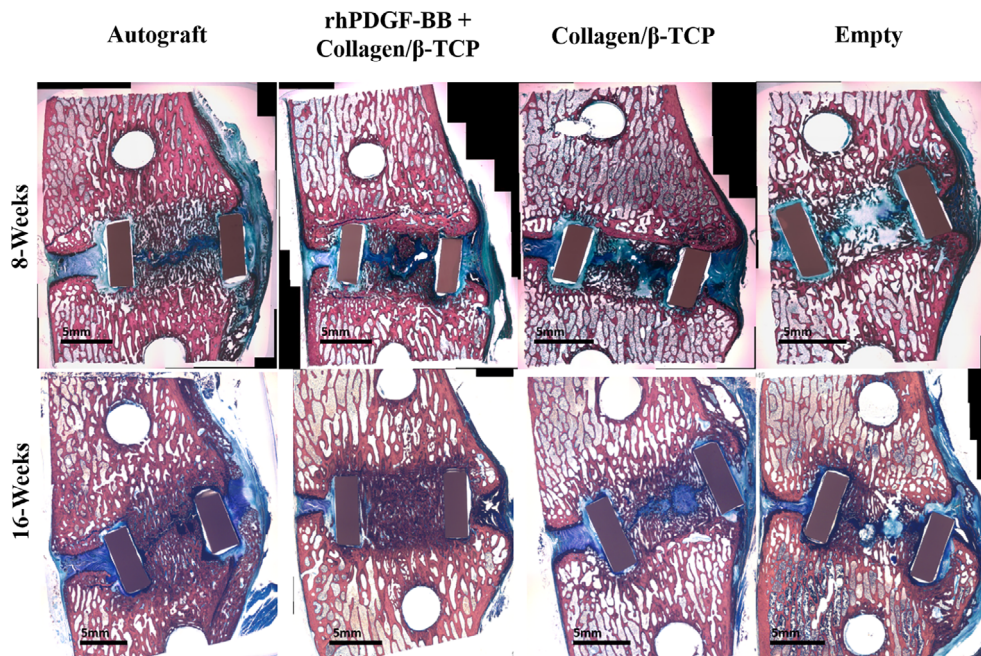
FIGURE 3 Representative sagittal plane histological images of bone formation within the interbody cage for each group at 8-week and 16-week timepoints. Note that specimens displayed match μCT specimens displayed in Figure 1. Pink/red stain = bone tissues, blue stained regions = soft fibrous/cartilage tissues

Similar levels of osteoblast and osteoclast activity were observed along new bone surfaces across all treatment groups at the 8-week timepoint and subsided by 16-weeks. Both osteoblasts and osteoclasts lined trabecular bone surfaces in similar numbers across all treatments at 8-weeks which again subsided similarly across treatments by the 16-week timepoint.

Localized inflammatory responses within treated defects was primarily associated with reactive fibrous tissue filling intertrabecular spaces of new bone or surrounding interbody cages and was similar in response level across all treatments at the 8-week timepoint with a downward trend in response after 16 weeks. Fibrosis and neovascularization of fibrous tissue was similar across all treatment groups at the 8- and 16-week timepoints. The histopathology data suggests that bone healing progressed similarly and normally for all animals and across all treatments over the course of the study.

4 | DISCUSSION

RhPDGF-BB combined with β-TCP and rhPDGF-BB combined with β-TCP/collagen matrix has been used to enhance bone healing extensively in the clinical context of hindfoot and ankle arthrodesis[9,15]; however, questions remain regarding its use as a viable alternative to autograft bone for spinal fusion. Autogenous bone graft remains the gold standard for human spinal surgery procedures. While this treatment is common, numerous limitations exist that support the need for alternative and effective treatment options. Autograft material is typically harvested from the patient's iliac crest and has been shown to result in patient complications unrelated to the primary spinal fusion procedure including infection, prolonged wound drainage, hematoma, pain lasting longer than 6 months, sensory loss, joint subluxation and destabilization, gait abnormalities, and pelvis/iliac fracture.[20,21,28-31] This study evaluated the efficacy of rhPDGF-BB combined with collagen/β-TCP in a sheep spinal fusion model using statistically meaningful sample sizes and comprehensive quantitative outcome measures that include kinematic, radiographic, and histological techniques. The data from this study indicate that rhPDGF-BB combined with collagen/β-TCP accelerates early bone formation as compared to collagen/β-TCP matrix without rhPDGF-BB or the use of an empty interbody spacer and promotes similar rates of bone formation at early and later timepoints as compared to autograft bone. Additionally, rhPDGF-BB combined with collagen/β-TCP promotes improved bone density at later timepoints as compared to collagen/β-TCP treatment alone.

Quantitative μCT and histological assessment demonstrated similar quantities of bone for all treatments at the 16-week timepoint. Despite similar amounts of bone for all treatments at this timepoint, bone quality (μCT bone density fraction) was significantly improved in animals that received either rhPDGF-BB + collagen/β-TCP or autograft treatment as compared to animals that did not. As bone volume fraction approaches 100% and bone density fraction approaches unity, then the ROI is considered to have a more solid architecture. At the earlier 8-week timepoint, bone quantity and quality did not differ between animals that received rhPDGF-BB + collagen/β-TCP or autograft treatment, while animals that were treated with collagen/β-TCP alone demonstrated significantly less histological bone area as compared to autograft animals. Despite the similar quantity of bone in rhPDGF-BB + collagen/β-TCP and autograft animals at 8-weeks, histological soft tissue area (comprised of a mixture of fibrosis, hyaline and fibro-cartilage) measured via histomorphometry analysis was significantly greater following rhPDGF-BB + collagen/β-TCP treatment as compared to autograft treatment. This increase in soft tissue content of rhPDGF-BB + collagen/β-TCP animals at 8-weeks suggests an
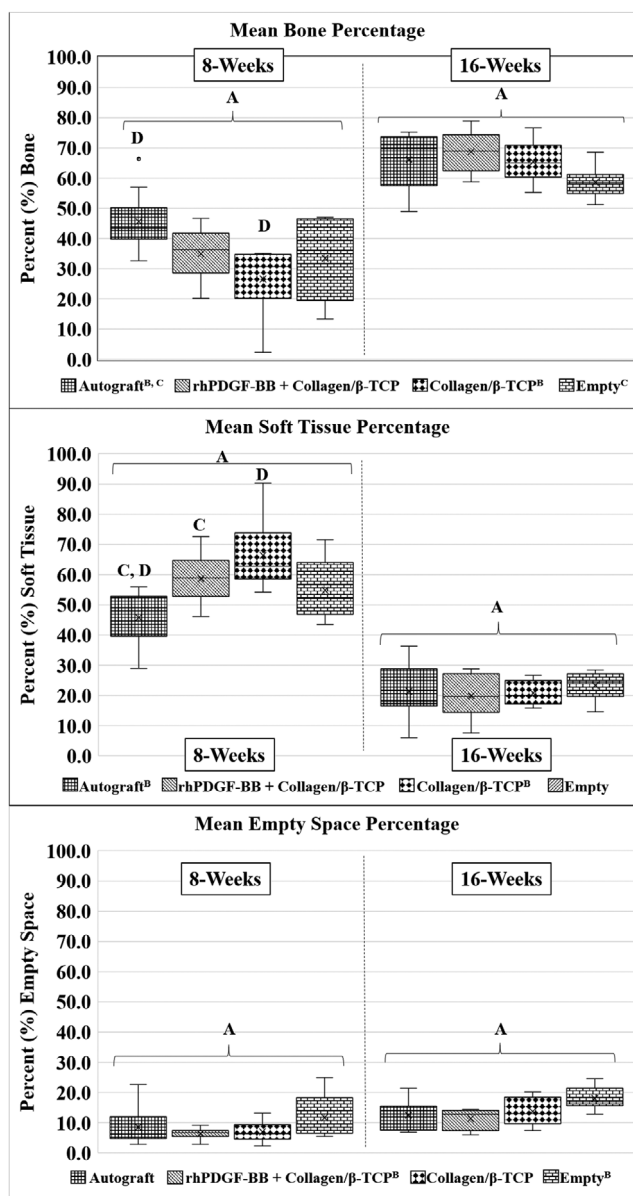
FIGURE 4   Quantitative two-dimensional histomorphometry analysis was performed within the area encompassed by the PEEK interbody cage. Like roman numerals presented in the figure or figure legend indicate statistical differences. (Top) Autograft treatment demonstrated significantly increased bone area as compared to collagen/β-TCP treatment at 8 weeks. No other statistically significant differences were observed between treatment groups within the 8-week or 16-week timepoints. Statistically significant overall main effects were observed between timepoints (greater bone area at 16-weeks as compared to 8-weeks, A: $P < .001$) and between treatment groups independent of timepoint where Autograft treatment resulted in increased bone area as compared to collagen/β-TCP (B: $P = .026$) and Empty cage (C: $P = .026$) treatments. (Middle) Soft tissue area was significant greater in rhPDGF-BB + collagen/β-TCP and collagen/β-TCP specimens as compared to Autograft specimens at 8-weeks (C: $P = .022$ and D: $P < .001$, respectively). No further statistical differences were observed between treatment groups within the 8-week or 16-week timepoints. Again, statistically significant overall main effects were observed between timepoints (greater soft tissue area at 8-weeks as compared to 16-weeks, A: $P < .001$) and between treatment groups independent of timepoint where Autograft treatment resulted in decreased soft tissue area as compared to collagen/β-TCP treatment (B: $P = .009$). (Bottom) No statistically significant differences were observed in the amount of empty space within the interbody cage between treatment groups within either timepoint. Statistically significant overall main effects were observed between timepoints (greater empty area at 16-weeks as compared to 8-weeks, A: $P < .001$) and between treatment groups independent of timepoint where rhPDGF-BB + collagen/β-TCP treatment resulted in decreased empty area as compared to Empty cage treatment (B: $P = .004$). Data are presented in box and whisker plot format. The "box" is bounded by the first and third quartiles and were generated exclusive of median values in the event there was an odd number of data points (Microsoft Excel 2016, Redmond, Washington). The "whiskers" represent the maximum/minimum values within the data set; the horizontal line represents the data median, and mean data are represented by "**x**." Outlier data are represented by "•" and were calculated as the first quartile minus 1.5 times the interquartile range or the third quartile plus 1.5 times the interquartile range, are highlighted
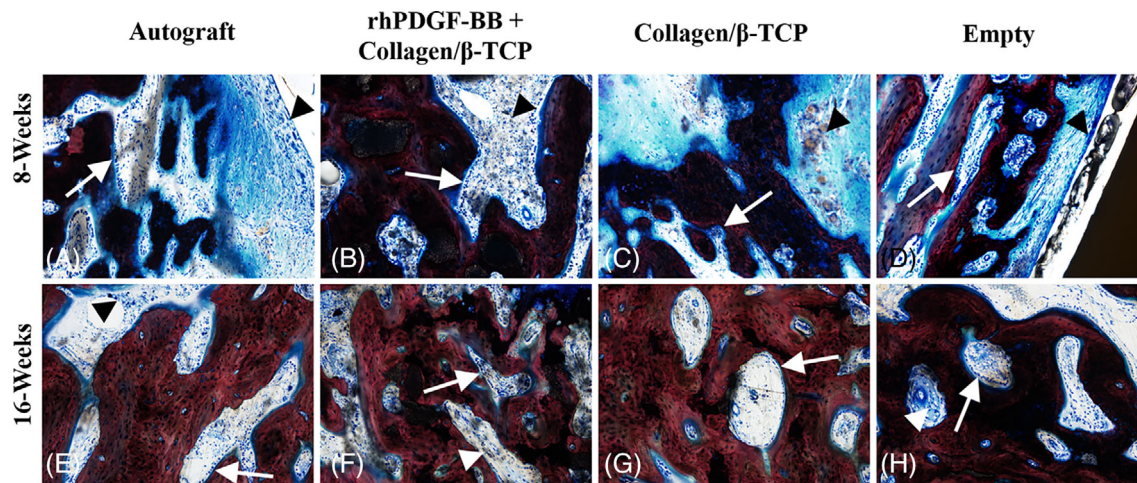
FIGURE 5 Histopathological assessment of host cell type and response. A-D, Representative photomicrographs of osteoblast activity and inflammation observed at the 8-week timepoint captured from the newly produced bone and associated soft tissue centrally present in the intervertebral defect space between the dorsal and ventrally visible aspects of the interbody cage. Images demonstrate numerous plump osteoblasts lining endosteal surfaces of new bone (white arrows). Inflammation in these animals was typically confined to the reactive fibrous tissue filling intertrabecular spaces of new bone and surrounding the implant and was composed of low to moderate numbers of macrophages, lymphocytes, and plasma cells (arrowheads). The degree of inflammation was greatest in the rhPDGF-BB + collagen/β-TCP, collagen/β-TCP, and empty specimens. E-H, Representative photomicrographs of osteoblast activity and inflammation observed in animals at the 16-week timepoint. Osteoblast activity (white arrows) was similar across all groups at this timepoint and was mildly decreased as compared to the 8-week timepoint. Similarly, while the cellular composition of the inflammatory infiltrate was similar, the degree of severity was similar across all groups at the 16-week timepoint, and uniformly decreased as compared to 8-week animals. All images 10× magnification

acceleration of the bone healing cascade resulting in greater rates of bone formation and improved bone quality observed at the later timepoint in the study, given the increased osteoblast recruitment observed in rhPDGF-BB + collagen/β-TCP animals as compared to autograft animals, and that both fibrous tissue and cartilage can serve as effective intermediates to promote endochondral ossification. It is important to note limitations in the ability to fully detect differences between bone and residual TCP particles with μCT due to similarities in attenuation properties of the two materials; however, this potential measurement artifact was controlled by including the animal cohort treated with collagen/TCP matrix alone to provide the baseline contribution of TCP to the μCT signal at each timepoint. Additionally, trends in bone content between treatment groups were similar between the μCT and histologic analysis modalities.

Biomechanically, functional fusion properties (ROM, neutral zone, stiffness) did not demonstrate statistical differences between treatment groups despite significant differences in μCT and histologic outcomes. This finding may be due to the fact that while differences in the quality of bone were improved due to rhPDGF-BB + collagen/β-TCP and autograft treatment as compared to collagen/β-TCP and empty PEEK cage treatment, the bone formed by the latter two treatment groups was sufficient to demonstrate comparable functional performance. More rigorous biomechanical testing scenarios such as fatigue, impact (and the resultant high specimen loading), or destructive biomechanical testing may demonstrate differences above what was observed with this low-cycle quasi-static experimental testing protocol. Additionally, since one purpose of an interbody fusion cage is to directly contribute to improved spinal stability in spinal fusion procedures, this may have masked the true effects of each treatment. To minimize the stability contributions of the interbody implants, appropriately sized implants were used, and the intervertebral space was widened during each procedure by removing a portion of the intervertebral body endplates to accommodate the implants. The density of the sheep bone used in preclinical orthopedic investigations is typically much greater than that of the target human population for these treatments, and the removal of tissue from the endplates allows for a closer representation of clinical human vertebral bone.[32] It is known that decorticating the bone leads to greater bone formation, therefore removal of tissue from the endplates may have increased the bone formation for all treatments and encouraged callus bone growth around the anterior region of the vertebral body and interbody cage.[33-35] It is also possible that preservation of the intervertebral endplates may have resulted in decreased bone growth, particularly in sham control animals. While the interbody cages were implanted as uniformly as possible, some slight variability in the final placement of the interbody cages is inherent due to the manual implantation process. Thus, inclusion of sham, "empty" cage controls was essential to the experimental design to provide visibility on the natural pace of bone healing following endplate decortication in this ovine model and how it compared to treatment with the test articles. Additionally, removal of the endplates allowed for the direct investigation of interbody cages sized for human clinical use which would not be possible if the endplates were preserved due to relatively small height of the sheep intervertebral disc (approximately 3-4 mm). Despite these precautions, the possibility of the interbody implants affecting the biomechanical results cannot be disregarded.

The results obtained in this study agree with previous studies performed investigating the effectiveness of rhPDGF-BB on bone formation. A previous study investigated the use of rhPDGF-BB combined with β-TCP or collagen/β-TCP for ovine lumbar interbody fusion after 24 weeks of healing.[23] The study concluded that rhPDGF-BB-containing treatment groups resulted in statistically improved fusion rates as compared to empty interbody cage implants and equivalent fusion rates as compared to autograft treatment. Mean μCT bone volume fraction values from this previous study for the autograft, rhPDGF-BB combined with β-TCP, and empty treatments were 67%, 63% to 76%, and 64%, respectively, while the current study resulted in μCT bone volume fraction values for the autograft, rhPDGF-BB combined with β-TCP, and empty treatments of 74%, 71%, and 59%, respectively. It should be noted that the previous study was limited to semi-quantitative μCT and histological fusion scoring performed at a single time point of 24 weeks. Nevertheless, the outcome of the current study compares favorably to this previous work and advances insight into the effect of treatment with rhPDGF-BB combined with collagen/β-TCP at earlier stages of lumbar bone healing, *ie.* 8 and 16 weeks. Other studies have produced similar results when investigating rhPDGF-BB + collagen/β-TCP for bone healing, particularly in vertebral body bone augmentation, and femoral and tibial fracture repair. Further, mineralized femoral fracture callus area and biomechanical strength was significantly improved in diabetic rat femoral fractures treated with rhPDGF-BB + collagen/β-TCP as compared to fractures that received no treatment or sham treatment.[13] Clinically, rhPDGF-BB + collagen/β-TCP or rhPDGF-BB + β-TCP treatment has been shown to be as effective and safe as the use of autogenous bone graft treatment in the context of foot and ankle fusion[36] and those effectiveness results corroborate the findings of the current study.

The use of animal models to investigate the effects of orthopedic treatments in humans remains a major limitation of preclinical studies due to differences in posture (biped vs quadruped), mechanical loading, and bone healing rates. However, the similarities in anatomical characteristics, *in vivo* biomechanical loading, bone composition, and bone architecture between humans and sheep make the ovine spinal fusion model one of the most relevant *in vivo* spine models in preclinical research.[37-41] The results of this study indicate that the use of rhPDGF-BB combined with collagen/β-TCP promotes spinal fusion comparably to that of autograft bone. Additionally, given its ability to promote spinal fusion in the ovine model, provides evidence for the potential safe and effective use of rhPDGF-BB combined with collagen/β-TCP in close proximity to the spine and spinal cord in other vertebrate mammals. Future clinical trials are needed to fully understand the effects of rhPDGF-BB + collagen/β-TCP on safety and effectiveness outcomes, and quality of life in human spinal fusion. In conclusion, these data indicate that rhPDGF-BB combined with collagen/β-TCP promotes spinal fusion comparably to autograft bone treatment and may offer a viable alternative in spinal fusion procedures. Future prospective clinical studies are necessary to fully understand the role of rhPDGF-BB combined with collagen/β-TCP in human spinal fusion healing.

AUTHOR CONTRIBUTIONS

Benjamin C. Gadomski participated in conceptual design of the study, data acquisition, analysis, interpretation, manuscript drafting, and final approval. Kevin M. Labus participated in data acquisition, analysis, interpretation, manuscript drafting, and final approval. Christian M. Puttlitz participated in conceptual design of the study, manuscript drafting, and final approval. Kirk C. McGilvray participated in conceptual design of the study, manuscript drafting, and final approval. Daniel P. Regan participated in data acquisition, analysis, interpretation, manuscript drafting, and final approval. Brad Nelson participated in conceptual design of the study, manuscript drafting, and final approval. Howard B. Seim III participated in conceptual design of the study, manuscript drafting, and final approval. Jeremiah T. Easley participated in conceptual design of the study, data acquisition, analysis, interpretation, manuscript drafting, and final approval. All authors agree to be accountable for this work and ensure its integrity.

ORCID

Benjamin C. Gadomski https://orcid.org/0000-0003-1434-0551
Christian M. Puttlitz https://orcid.org/0000-0002-1255-8867

REFERENCES

1. Fiedler J, Etzel N, Brenner RE. To go or not to go: migration of human mesenchymal progenitor cells stimulated by isoforms of PDGF. *J Cell Biochem*. 2004;93(5):990-998.
2. Mehrotra M, Krane SM, Walters K, Pilbeam C. Differential regulation of platelet-derived growth factor stimulated migration and proliferation in osteoblastic cells. *J Cell Biochem*. 2004;93(4):741-752.
3. Ozaki Y, Nishimura M, Sekiya K, et al. Comprehensive analysis of chemotactic factors for bone marrow mesenchymal stem cells. *Stem Cells Dev*. 2007;16(1):119-129.
4. Caplan AI, Correa D. PDGF in bone formation and regeneration: new insights into a novel mechanism involving MSCs. *J Orthop Res*. 2011;29(12):1795-1803.
5. Peng Y, Wu S, Li Y, Crane JL. Type H blood vessels in bone modeling and remodeling. *Theranostics*. 2020;10(1):426-436.
6. Wang X, Matthews BG, Yu J, et al. PDGF modulates BMP2-induced Osteogenesis in periosteal progenitor cells. *JBMR Plus*. 2019;3(5):e10127.
7. Xie H, Cui Z, Wang L, et al. PDGF-BB secreted by preosteoclasts induces angiogenesis during coupling with osteogenesis. *Nat Med*. 2014;20(11):1270-1278.
8. DiGiovanni CW, Lin S, Pinzur M. Recombinant human PDGF-BB in foot and ankle fusion. *Expert Rev Med Devices*. 2012;9(2):111-122.
9. DiGiovanni CW, Lin SS, Baumhauer JF, et al. Recombinant human platelet-derived growth factor-BB and beta-tricalcium phosphate (rhPDGF-BB/β-TCP): an alternative to autogenous bone graft. *JBJS*. 2013;95(13):1184-1192.

10. Krell ES, DiGiovanni CW. The efficacy of platelet-derived growth factor as a bone-stimulating agent. *Foot Ankle Clin*. 2016;*21*(4):763-770.

11. Nash TJ, Howlett CR, Martin C, Steele J, Johnson KA, Hicklin DJ. Effect of platelet-derived growth factor on tibial osteotomies in rabbits. *Bone*. 1994;*15*(2):203-208.

12. Hollinger JO, Onikepe AO, MacKrell J, et al. Accelerated fracture healing in the geriatric, osteoporotic rat with recombinant human platelet-derived growth factor-BB and an injectable beta-tricalcium phosphate/collagen matrix. *J Orthop Res*. 2008;*26*(1):83-90.

13. Al-Zube L, Breitbart EA, O'Connor JP, et al. Recombinant human platelet-derived growth factor BB (rhPDGF-BB) and beta-tricalcium phosphate/collagen matrix enhance fracture healing in a diabetic rat model. *J Orthop Res*. 2009;*27*(8):1074-1081.

14. Mitlak BH, Finkelman RD, Hill EL, et al. The effect of systemically administered PDGF-BB on the rodent skeleton. *J Bone Miner Res*. 1996;*11*(2):238-247.

15. Daniels TR, Younger AS, Penner MJ, et al. Prospective randomized controlled trial of Hindfoot and ankle fusions treated with rhPDGF-BB in combination with a beta-TCP-collagen matrix. *Foot Ankle Int*. 2015;*36*(7):739-748.

16. Berlet GC, Baumhauer JF, Glazebrook M, et al. The impact of patient age on foot and ankle arthrodesis supplemented with autograft or an autograft alternative (rhPDGF-BB/beta-TCP). *JB JS Open Access*. 2020;*5*(4).

17. Rajaee SS, Bae HW, Kanim LE, Delamarter RB. Spinal fusion in the United States: analysis of trends from 1998 to 2008. *Spine*. 2012;*37*(1):67-76.

18. Kuslich SD, Ulstrom CL, Griffith SL, Ahern JW, Dowdle JD. The Bagby and Kuslich method of lumbar interbody fusion: history, techniques, and 2-year follow-up results of a United States prospective, multicenter trial. *Spine*. 1998;*23*(11):1267-1278.

19. McAfee PC, Boden SD, Brantigan JW, et al. Symposium: a critical discrepancy—a criteria of successful arthrodesis following interbody spinal fusions. *Spine*. 2001;*26*(3):320-334.

20. Fowler B, Dall B, Rowe D. Complications associated with harvesting autogenous iliac bone graft. *Am J Orthop*. 1995;*24*(12):895-903.

21. Goulet JA, Senunas LE, DeSilva GL, Greenfield MLV. Autogenous iliac crest bone graft: complications and functional assessment. *Clin Orthop Relat Res*. 1997;*339*:76-81.

22. Perrien DS, Young CS, Alvarez-Urena PP, Dean DD, Lynch SE, Hollinger JO. Percutaneous injection of augment injectable bone graft (rhPDGF-BB and beta-tricalcium phosphate [beta-TCP]/bovine type I collagen matrix) increases vertebral bone mineral density in geriatric female baboons. *Spine J*. 2013;*13*(5):580-586.

23. Solchaga LA, Hee CK, Aguiar DJ, et al. Augment bone graft products compare favorably with autologous bone graft in an ovine model of lumbar interbody spine fusion. *Spine*. 2012;*37*(8):E461-E467.

24. Nevins M, Giannobile WV, McGuire MK, et al. Platelet-derived growth factor stimulates bone fill and rate of attachment level gain: results of a large multicenter randomized controlled trial. *J Periodontol*. 2005;*76*(12):2205-2215.

25. Sarment DP, Cooke JW, Miller SE, et al. Effect of rhPDGF-BB on bone turnover during periodontal repair. *J Clin Periodontol*. 2006;*33*(2):135-140.

26. DiGiovanni CW, Lin SS, Baumhauer JF, et al. Recombinant human platelet-derived growth factor-BB and beta-tricalcium phosphate (rhPDGF-BB/beta-TCP): an alternative to autogenous bone graft. *J Bone Joint Surg Am*. 2013;*95*(13):1184-1192.

27. Smit TH, van Tunen MS, van der Veen AJ, Kingma I, van Dieen JH. Quantifying intervertebral disc mechanics: a new definition of the neutral zone. *BMC Musculoskelet Disord*. 2011;*12*:38.

28. Almaiman M, Al-Bargi HH, Manson P. Complication of anterior iliac bone graft harvesting in 372 adult patients from may 2006 to may 2011 and a literature review. *Craniomaxillofac Trauma Reconstr*. 2013;*6*(4):257-266.

29. Dosoglu M, Orakdogen M, Tevruz M, Gogusgeren MA, Mutlu F. Enterocutaneous fistula: a complication of posterior iliac bone graft harvesting not previously described. *Acta Neurochir*. 1998;*140*(10):1089-1092.

30. Fernando TL, Kim SS, Mohler DG. Complete pelvic ring failure after posterior iliac bone graft harvesting. *Spine*. 1999;*24*(20):2101-2104.

31. Younger EM, Chapman MW. Morbidity at bone graft donor sites. *J Orthop Trauma*. 1989;*3*(3):192-195.

32. Aerssens J, Boonen S, Lowet G, Dequeker J. Interspecies differences in bone composition, density, and quality: potential implications for in vivo bone research. *Endocrinology*. 1998;*139*(2):663-670.

33. Chen L, Liu HL, Gu Y, Feng Y, Yang HL. Lumbar interbody fusion with porous biphasic calcium phosphate enhanced by recombinant bone morphogenetic protein-2/silk fibroin sustained-released microsphere: an experimental study on sheep model. *J Mater Sci Mater Med*. 2015;*26*(3).

34. Grgurevic L, Erjavec I, Gupta M, et al. Autologous blood coagulum containing rhBMP6 induces new bone formation to promote anterior lumbar interbody fusion (ALIF) and posterolateral lumbar fusion (PLF) of spine in sheep. *Bone*. 2020;*138*:115448.

35. Pobloth AM, Duda GN, Giesecke MT, Dienelt A, Schwabe P. High-dose recombinant human bone morphogenetic protein-2 impacts histological and biomechanical properties of a cervical spine fusion segment: results from a sheep model. *J Tissue Eng Regen Med*. 2017;*11*(5):1514-1523.

36. Sun H, Lu PP, Zhou PH, et al. Recombinant human platelet-derived growth factor-BB versus autologous bone graft in foot and ankle fusion: a systematic review and meta-analysis. *Foot Ankle Surg*. 2017;*23*(1):32-39.

37. Wilke HJ, Kettler A, Claes LE. Are sheep spines a valid biomechanical model for human spines? *Spine*. 1997;*22*(20):2365-2374.

38. Wilke HJ, Kettler A, Wenger KH, Claes LE. Anatomy of the sheep spine and its comparison to the human spine. *Anat Rec*. 1997;*247*(4):542-555.

39. Sheng SR, Wang XY, Xu HZ, Zhu GQ, Zhou YF. Anatomy of large animal spines and its comparison to the human spine: a systematic review. *Eur Spine J*. 2010;*19*(1):46-56.

40. Pearce AI, Richards RG, Milz S, Schneider E, Pearce SG. Animal models for implant biomaterial research in bone: a review. *Eur Cell Mater*. 2007;*13*:1-10.

41. Kettler A, Liakos L, Haegele B, Wilke HJ. Are the spines of calf, pig and sheep suitable models for pre-clinical implant tests? *Eur Spine J*. 2007;*16*(12):2186-2192.